Philosophical Transactions of The Royal Society B

Regulatory mechanisms underlying the specification of the pupal-homologous stage in a hemimetabolous insect

Yoshiyasu Ishimaru[1], Sayuri Tomonari[2], Takahito Watanabe[1], Sumihare Noji[1], and Taro Mito[1]*

[1]Division of Bioscience and Bioindustry, Graduate School of Technology, Industrial and Social Sciences, Tokushima University, 2-1 Minami-Jyosanjima-cho, Tokushima City, Tokushima 770-8513, Japan

[2] Division of Chemical and Physical Analyses, Center for Technical Support, Institute of Technology and Science, Tokushima University, 2-1 Minami-Jyosanjima-cho, Tokushima City, Tokushima 770-8506, Japan

*Corresponding author

Correspondence should be sent to:

Dr Taro Mito, Division of Bioscience and Bioindustry, Graduate School of

Technology, Industrial and Social Sciences, Tokushima University, 2-1 Minami-Jyosanjima-cho, Tokushima City, Tokushima 770-8513, Japan
Tel: +81-88-656-7529; E-mail: mito.taro@tokushima-u.ac.jp

Running head: Regulation of cricket metamorphosis

Running title: Respective roles of Kr-h1, Br and E93 in hemimetabolous metamorphosis

Abstract

Juvenile hormones (JHs) and the genetic interaction between the transcription factors *Krüppel homolog 1* (*Kr-h1*) and *Broad* (*Br*) regulate the transformation of insects from immature to adult forms in both types of metamorphosis (holometaboly with a pupal stage versus hemimetaboly with no pupal stage); however, knowledge about the exact instar in which this occurs is limited. Using the hemimetabolous cricket *Gryllus bimaculatus* (*Gb*), we demonstrate that a genetic interaction occurs among *Gb'Kr-h1*, *Gb'Br* and the adult-specifier transcription factor *Gb'E93* from the sixth to final (eighth) nymphal instar. *Gb'Kr-h1* and *Gb'Br* mRNAs were strongly expressed in the abdominal tissues of sixth instar nymphs, with precocious adult moults being induced by *Gb'Kr-h1* or *Gb'Br* knockdown in the sixth instar. Depletion of *Gb'Kr-h1* or *Gb'Br* up-regulates *Gb'E93* in the sixth instar. In contrast, *Gb'E93* knockdown at the sixth instar prevents nymphs transitioning to adults, instead producing supernumerary nymphs. *Gb'E93* also represses *Gb'Kr-h1* and *Gb'Br* expression in the penultimate nymphal instar, demonstrating its important role in adult differentiation. Our results suggest that the regulatory mechanisms underlying the pupal transition in holometabolous insects are evolutionarily conserved in hemimetabolous *G. bimaculatus*, with the penultimate and final nymphal periods being equivalent to the pupal stage.

Keywords: *Gryllus bimaculatus*, insect metamorphosis, Krüppel homolog 1, Broad complex, E93.

1. Introduction

Holometabolous insects, such as butterflies, beetles and flies, undergo a complete morphological transformation from larva to adult via a pupal stage. The intermediate pupal stage is specific to holometabolous insects, and is needed to transform immature larvae to winged adults. The nymphs of hemimetabolous insects, like locusts, cockroaches and crickets, also undergo morphogenesis to form mature wings and external genitalia, as observed in the larva-to-pupa transition and pupa of holometabolous insects. However, the nymphs of hemimetabolous insects resemble miniature adult forms with wing pads, with the wings and genitalia outgrowths developing throughout the nymphal stages.

Despite these two types of metamorphosis being clearly distinct, both are regulated by two hormones, the steroid 20-hydroxyecdysone (20E) and the sesquiterpenoid juvenile hormones (JHs)[1-3]. 20E is the most active form of insect molting hormone, ecdysone, and larval-larval molting and larval-pupal-adult metamorphosis are provoked by pulses of 20E[4,5]. 20E binds to a heterodimer in the nuclear receptor complex, ecdysone receptor (EcR) and ultraspiracle protein (USP), and EcR-USP binds to 20E response elements (EcRE). 20E-EcR-USP triggers a transcriptional cascade, which include transcription of the 20E primary response genes, such as *Br-C*, *E74*, *E75*, and *E93*, and subsequent events of 20E secondary response genes[4,5]. However, the type of moult is determined by JH levels. For instance, for

larva-to-larva moults, high JH titres are needed. JH antagonizes 20E signaling to prevent precocious metamorphosis during the larval stages, and the metamorphic moult occurs when the JH titre drops during the final instar. JH acting through JH receptor MET (Methoprene-tolerant)[6-9], which is the bHLH-PAS protein family member, prevents adult differentiation during the pre-ultimate immature stages, by inducing the expression of the antimetamorphic transcription factor gene *Krüppel-homolog 1* (*Kr-h1*)[3,10-13]. JH-stimulated *Kr-h1* expression prevents metamorphosis, whereas the noticeable decline in *Kr-h1* expression, following a natural drop in the JH titre during the final juvenile stages, particularly last-instar nymphs in hemimetabolans and pupae in holometabolans, permits adult development[14-18].

A key regulatory gene in the metamorphosis of holometabolous insects is the pupal-specifier transcription factor *Broad* (*Br*), which specifies pupal development. The transient expression of *Br* is essential for the successful formation of pupae. The subsequent repression of *Br* during the pupal stage allows proper pupal–adult transition[19-22]. In *Drosophila melanogaster* (*Dm*), *Dm'Br* is predominantly expressed during the larval-pupal transition when 20E is high and JH is absent[23,24]. In comparison, the milkweed bug *Oncopeltus fasciatus* (*Of*) and cockroach *Blattella germanica* (*Bg*), which are hemimetabolous insects that lack pupal stages, *Of'Br* or *Bg'Br* are expressed during embryonic, pronymphal (first postembryonic

form before hatching) and nymphal development, but then disappear at the moult to adult[25,26]. However, during the final nymphal instar of *B. germanica* nymphal instar, a small peak in *Bg'Br* expression was reported when ecdysone peaks. Thus, these compounds, at least, regulate gradual wing bud growth.

Recent studies have identified *E93*, which is a helix–turn–helix transcription factor containing a Pipsqueak (Psq) motif, as an important player downstream of *Kr-h1*[27]. Depletion of *E93* in final instar nymphs of *B. germanica*, as well as the pupae of *Tribolium castaneum* (*T. castaneum*) and *D. melanogaster,* prevents transition to the adult stage. Thus, in contrast to *Kr-h1*, it has been proposed that *E93* is an adult specifier in both hemimetabolan and holometabolan species[28,29]. The effects of *Kr-h1* and *E93* are, to some extent, antagonistic during the prefinal nymphal instars of *B. germanica*, with *Kr-h1* and *E93* acting as mutual repressors[28].

Based on experimental data of *B. germanica*, *T. castaneum* and *D. melanogaster*, Bellés and Santos[30,31] proposed the MEKRE93 (Met-Kr-h1-E93) pathway to explain the regulation of insect metamorphosis. The MEKRE93 pathway appears to be central to the status quo action of JH, which switches adult morphogenesis off and on in a variety of insect species, ranging from cockroaches to flies. JH signals through Met to induce the expression of *Kr-h1*, which, in turn, blocks adult development, at least partly, by repressing the *E93* gene.

The single short period of morphogenesis that arises in the larva-to-pupa transition of holometabolous insects evolved from progressive changes that occur during the nymphal series in basal insects. The hemimetabolous *B. germanica* and Hemiptera (true bugs) pass through six and five instar stages, respectively, before becoming adults. The levels of *Kr-h1* mRNA in these insects are not detectable in the final nymphal stage, which allows adult development. In addition, *Br* levels are greatly reduced during the final instar.

To extend our further understanding of the conservation and diversification in the mechanisms of metamorphosis among hemimetabolous insects, this study focused on the two-spotted cricket, *Gryllus bimaculatus*, belonging to the order Orthoptera. In *G. bimaculatus* nymphs, the life stages following hatching progresses through eight instars, moulting into adults after the final (eighth) instar nymph[32,33]. Based on the MEKRE93 pathway, we propose a model to explain the evolution of pupal formation. In the hemimetabolous *G. bimaculatus*, RNA interference (RNAi)-mediated knockdown of *Gb'Kr-h1* or *Gb'Br* during the nymphal stage causes the precocious up-regulation of *Gb'E93* and adult differentiation, bypassing the penultimate and the final nymphal instar stages. In addition to *Gb'Kr-h1* and *Gb'Br*, we show that *Gb'E93* is highly expressed in the penultimate nymphal instar, with RNAi knockdown of *Gb'E93* preventing nymphal–adult transition, inducing an endless reiteration of nymphal development. Based on our findings, we propose a novel hypothesis for the evolutionary origin

of the pupal homologous stage in the hemimetabolous insect, *G. bimaculatus*.

2. Material and methods

(a) Animals

All adults and nymphs of the two-spotted cricket, *G. bimaculatus*, were reared at 28 ℃ and 70% under standard conditions, as described previously[34].

(b) Cloning

Gryllus cDNAs homologous to *Kr-h1* (346bp) and *Br* (978bp) or *E93* (1572bp) were cloned by RT-PCR from abdomen cDNA samples of third or eighth instar nymphs, respectively, by using gene-specific primers listed in Table S3. The design of all gene-specific primers was performed with the draft genomic sequences of *G. bimaculatus* (Mito et al., unpublished). All PCR conditions were as follows: 98 °C for 2.5 min, 40 cycles of 94 °C for 30 s, 55 °C for 30 s, and 72 °C for 1 min, followed by 72 °C for 5 min. Following amplification, the PCR products were subcloned into a pGEM T-Easy vector (Promega, Madison, WI, USA) and were sequenced using an ABI-300 instrument (Applied Biosystems, Foster City, CA, USA). Recombinant vector containing the *Gb'Kr-h1* cDNA fragment was used for dsRNA synthesis.

(c) RNA interference (RNAi)

Template cDNA fragments for the synthesis of *Gb'Br* and *Gb'E93* dsRNAs were prepared by RT-PCR by using gene-specific primers listed in Table S4.

The templates for *Gb'Kr-h1* (346bp), *Gb'Br* (448bp) and *Gb'E93* (492bp) dsRNA synthesis were amplified with a T7 promoter sequence primer and a Sp6 promoter sequence primer with T7 on the 5' end. dsRNAs were synthesised using the MEGAscript T7 Transcription Kit (Ambion, Austin, TX, USA). Within 24 h of ecdysis, nymphs were injected in the ventral abdomen with 20 μM dsRNA in a volume of 0.2–0.5 μl, as described previously[35]. In all RNAi experiments, *DsRed2* dsRNA was injected as a negative control, as described previously[36]. The body length (cm) of RNAi-treated adults was measured from the anterior part of the head to the posterior of the anus, and weight (gram) was measured in the whole body just after moulting to adult. The graphs of body size are created using the average values of measured body length and weight in each RNAi-treated adult. The obtained total numbers of survival are shown in Table S1 and S2.

(d) Quantitative RT-PCR (qPCR)

Total RNA was extracted from the abdomen tissues, including peripheral tissues such as epidermis and fat body cells targeted by JH and 20E[12,24,37], using ISOGEN (Wako Pure Chemical Industries Ltd., Osaka, Japan). Total RNA was reverse transcribed to cDNA using the SuperScript III First-Strand Synthesis System (Invitrogen, Carlsbad, CA, USA) with an oligo$(dT)_{20}$ primer, according to the manufacturer's instructions. The qPCR primers that were used are listed in Table S5. qPCR was performed using the Power

SYBR Green PCR Master Mix (Applied Biosystems, Foster City, CA, USA) on an ABI 7900 Real-Time PCR System (Applied Biosystems, Foster City, CA, USA). qPCR conditions were as follows: 95 °C for 10 min and then 95 °C for 15 s, 60 °C for 30 s and 72 °C for 30 s repeated 40 cycles with 0.4 μM concentration of each primer. The *G. bimaculatus β-actin* (*Gb'β-actin*) gene was detected as a reference gene. All qPCR reactions were performed in triplicate as technical replicates.

(e) Hormone treatment

20-hydroxyecdysone (20E, Sigma-Aldrich, Saint Louis, MO, USA) was dissolved in ethanol to a concentration of 1 μg/μl, and then approximately 3 μl of this 20E solution was injected into the ventral abdomen of newly moulted fifth instar nymphs (~3 μg of 20E/nymph). The same volume of ethanol was injected as a control.

3. Results

(a) *Gb'Kr-h1* and *Gb'Br* prevent adult metamorphosis during late instar stages of the hemimetabolous *Gryllus bimaculatus*

The cricket *G. bimaculatus* progresses through eight nymphal instars before adult differentiation, with each nymphal instar being distinguished by body size and shape (figure 1*a*). In particular, the morphological changes that occur between the sixth and the penultimate (seventh) instar are mainly characterised by the degree of development of the wing pads and ovipositor (electronic supplementary material, figure S1*a-d*). However, no significant changes were observed during the seventh and final (eighth) instar (electronic supplementary material, figure S1*c-f*). Following the injection of progressively younger fifth instar with dsRNA, we found that nymphs treated with RNAi against *Gb'Kr-h1* moulted into normal sixth instar nymphs, showing precocious differentiation of adult features in the ensuing moult, instead of moulting into seventh instar nymphs, as observed for control nymphs in both sexes (figure 1*b*; electronic supplementary material, Table S1). RNAi-mediated depletion of *Gb'Br* in fifth instar nymphs also caused precocious metamorphosis to adults, instead of normal moult to seventh instar (figure 1*c*; electronic supplementary material, Table S1). In addition, the overall body size and weight of the treated precocious adults significantly declined (figure 1*d*,*e*). These animals were not able to moult again, and exhibited strikingly abnormal morphology of the wings (figure

1*g*,*h*; electronic supplementary material, figure S2) and ovipositor (figure 1*k*,*l*), as compared with the control (figure 1*f*,*j*). Interestingly, when fifth instar nymphs were treated with 20E, precocious metamorphosis was induced after the sixth instar, instead of normal moult to seventh instar. In addition, the abnormal development of the wing and ovipositor resembled that of animals subjected to *Gb'Kr-h1* and *Gb'Br* RNAi (figure 1*i*,*m*). These results demonstrate that *Gb'Kr-h1* and *Gb'Br* are required for the seventh instar moult, and that their functions during the sixth instar are essential to prevent the precocious differentiation of adult features.

(b) *Gb'E93* promotes adult differentiation in the last instar stage

When *Gb'E93* dsRNA was injected into fifth instar nymphs, all *Gb'E93* RNAi nymphs successfully moulted to normal final instar nymphs, but subsequently failed to cause adult metamorphosis. Instead, the individuals of both sexes repeated the nymphal moult to the supernumerary instar. All of the supernumerary *Gb'E93* RNAi nymphs continuously moulted until they became giant tenth instar nymphs (figure 2*a*,*b*). Although the development of many of these supernumerary nymphs was arrested without adult metamorphosis, several individuals subsequently moulted into adults (figure 2*c*; electronic supplementary material, Table S2). However, instead of the normal adult pigmentation with a black cuticle, the supernumerary *Gb'E93* RNAi tenth instar nymphs had the typical

characteristics of control eighth instar nymphs. Specifically, they had thick lines of white melanin on the prothorax and head (figure 2*d-f*). Consistently, when nymphs moulted to the supernumerary tenth instar, their body size and weight were significantly larger than those of control adults (figure 2*g*,*h*). Furthermore, the wing pads of these tenth instar nymphs had similar proportions to those of eighth instar nymphs, and begin to bend to the outside (figure 2*i*,*j*). These *Gb'E93* knockdown experiments indicate that *Gb'E93* is required for the morphological transition from the eighth instar to adults. Thus, *Gb'E93* is a critical factor that promotes adult metamorphosis in hemimetabolous *G. bimaculatus*.

(c) Interplay between *Gb'Kr-h1*, *Gb'Br* and *Gb'E93* is associated with sixth instar-to-adult transition of *Gryllus bimaculatus*

Gb'Kr-h1 and *Gb'Br* mRNAs were found to be constitutively expressed throughout the nymphal stages, while the levels of these mRNAs exhibited periodic changes in each of the instars (figure 3*a*,*c*). The peak in relative amount of *Gb'Kr-h1* transcript was observed on day 1 of the sixth instar, but decreased until it could no longer be detected during the seventh instar (figure 3*b*). Similarly, higher *Gb'Br* mRNA level was detected in the sixth instar, and then mRNA level decreased during the seventh instar (figure 3*d*). Conversely, the expression of *Gb'E93* transcript significantly increased after moulting to the seventh instar, and the high transcript level was also

detected in the eighth instar (figure 3*e*,*f*). Declines in *Gb'Kr-h1* and *Gb'Br* expression, and an increased expression of *Gb'E93,* suggest that the cross talk between these genes contributes towards regulating metamorphosis in *G. bimaculatus* (figure 3*g*).

At the sixth instar, the level of *Gb'Kr-h1* mRNA in *Gb'Kr-h1* RNAi nymphs was significantly lower than that in the control (figure 4*a*). The knockdown of *Gb'Kr-h1* caused the mRNA level of *Gb'Br* to decline in comparison to the control (figure 4*b*). Thus, the expression of *Gb'Br* during the sixth instar might be controlled by *Gb'Kr-h1*. However, *Gb'E93* expression during the sixth instar was up-regulated by *Gb'Kr-h1* RNAi knockdown (figure 4*c*). Similarly, the RNAi-mediated depletion of *Gb'Br* (figure 4*b*) also caused the expression of *Gb'E93* to increase during the sixth instar when compared to its expression in the control (figure 4*c*). Thus, the *Gb'E93* transcript during the sixth instar had already been repressed by *Gb'Kr-h1* and *Gb'Br*.

Of note, the expression levels of *Gb'Kr-h1* and *Gb'Br* progressively declined during the seventh instar, just after *Gb'E93* up-regulation. When sixth instar nymphs received *Gb'E93* RNAi, *Gb'Br* mRNA levels in *Gb'E93* RNAi nymphs were significantly higher than those of control nymphs (figure 4*b*), despite *Gb'Kr-h1* not being up-regulated in these sixth instar nymphs (figure 4*a*). These results suggest that *Gb'Br* expression might be negatively affected by *Gb'E93* in the sixth instar nymphs. Accordingly, the precious

increase of *Gb'E93* expression caused by the RNAi-mediated *Gb'Kr-h1* knockdown might lead to reduced expression of *Gb'Br* during the sixth instar. Interestingly, under the *Gb'Br* RNAi treatment, *Gb'Kr-h1* expression during the sixth instar was down-regulated in these nymphs (figure 4*a*). Consequently, the observed decrease in *Gb'Kr-h1* might be due to increased *Gb'E93* expression, which results in *Gb'Br* knockdown. Thereafter, *Gb'E93* depletion during the seventh instar prevented the down-regulation of *Gb'Kr-h1* and *Gb'Br* (figure 4*d*). Thus, the *Gb'Kr-h1* and *Gb'Br* transcripts during the seventh instar can be tightly repressed by *Gb'E93*.

In previous studies in *D. melanogaster* and *Bombyx mori*[38-40], *E93* has been found to be a primary response gene that is positively regulated by 20E. In the present study, we showed that the injection of 20E into the fifth instar nymphs causes precocious metamorphosis to adults, instead of moulting into seventh instar nymphs. Consistent with the precocious adult metamorphosis that had received 20E treatment, *Gb'E93* mRNA levels were up-regulated at the sixth instar nymphs, while *Gb'Kr-h1* and *Gb'Br* were down-regulated (figure 4*e*). Thus, the expression of *Gb'E93* might be positively affected by an excess of 20E during the sixth instar.

Overall, our results indicate that the precocious adult moult in *Gb'Kr-h1* and *Gb'Br* RNAi nymphs depends on the precocious up-regulation of *Gb'E93* expression during the sixth instar. Furthermore, *Gb'E93* causes morphological changes to form adults through the repression of *Gb'Kr-h1*

and *Gb'Br* during the penultimate and final nymphal instars, as adult metamorphosis is prevented by RNAi depletion of *Gb'E93*.

(d) *Gb'Kr-h1*, *Gb'Br* and *Gb'E93* expression are influenced by JH biosynthesis signaling

Based on our recent study, *Gb*'Myoglianin (*Gb*'Myo) and *Gb*'Decapentaplegic (*Gb*'Dpp)/*Gb*'Glass bottom boat (*Gb*'Gbb) signaling are involved in JH synthesis by mediating the transcriptional regulation of *Gb'jhamt*[33]. *Gb'jhamt* is a key enzyme for JH biosynthesis in the corpora allata (CA) of *G. bimaculatus*. Because the RNAi-mediated depletion of *Gb*'Myo and *Gb*'Dpp/*Gb*'Gbb signaling molecules altered the JH titre to increase and decrease, respectively, we examined how the expression of *Gb'Kr-h1*, *Gb'Br* and *Gb'E93* is altered by *Gb'myo* or *Gb'mothers against dpp* (*Gb'mad*) knockdown.

We have previously shown that RNAi targeting *Gb'mad* results in significant reductions of *Gb'jhamt* transcript and JH titre in the sixth instar nymphs and consequently causes precocious adult metamorphosis[33]. Here we found that the levels of *Gb'Kr-h1* and *Gb'Br* mRNA in *Gb'mad* RNAi-treated nymphs were lower than those in the controls during the sixth instar (figure 5*a*,*b*). Thus, the decline of *Gb'Kr-h1* and *Gb'Br* mRNA levels might be largely attributed to the absence of JH by the depletion of *Gb'mad*. Furthermore, the knockdown of *Gb'mad* caused the expression of *Gb'E93*

to increase during the sixth instar (figure 5*c*). In contrast, *Gb'Kr-h1* and *Gb'Br* mRNA levels were up-regulated in *Gb'myo* RNAi nymphs during the sixth instar (figure 5*a*,*b*). Furthermore, we also found that *Gb'myo* RNAi allows the strong up-regulation of *Gb'E93* (figure 5*c*). Thus, *Gb'Kr-h1*, *Gb'Br-C* and *Gb'E93* are probably regulated by JH in hemimetabolous *G. bimaculatus*.

4. Discussion

Previous studies showed that the down-regulation of *Kr-h1* and the up-regulation of *E93* in the final nymph stages of hemimetabolous insects and in the pupae of holometabolous insects are crucial for adult development in both types of metamorphosis[14,29,30,31,41]. The present study showed that RNAi-mediated depletion of *Gb'Kr-h1* during the sixth nymphal instar of *G. bimaculatus* induces *Gb'E93* and suppresses *Gb'Br* expression. Consequently, *Gb'Kr-h1* RNAi animals showed the precocious differentiation of adult features. We also showed that RNAi knockdown of *Gb'E93* during the penultimate (seventh) nymphal instar prevents adult metamorphosis and promotes supernumerary nymphal moults. In addition, *Gb'E93* is required to prevent the expression of *Gb'Kr-h1* and *Gb'Br* during the penultimate nymphal instar. Overall, the mechanism of the functional interactions between *Kr-h1* and *E93* for metamorphosis is conserved in *G. bimaculatus*. Consequently, the regulation of MEKRE93 pathway is common throughout hemimetabolous and holometabolous insects. However, based on data reported from other hemimetabolous insects (including *Pyrrhocoris apterus*, *Rhodnius prolixus*, *Cimex lectularius* and *B. germanica*), changes to the timing of expression and regulation of cross-talk between *Kr-h1, Br* and *E93* usually occur during the penultimate and final nymphal period[14,17,29,42] as they do during the final larval and pupal stage in holometabolous insects. In comparison, the functional relationship between

Gb'Kr-h1, *Gb'Br* and *Gb'E93* is already present in the antepenultimate (sixth) instar nymphs of *G. bimaculatus*. Consequently, *Gb'Kr-h1* RNAi-dependent induction of *Gb'E93* expression during the sixth instar initiates the precocious development of adult structures. Previous reports showed that high JH levels prevent the incomplete metamorphosis, by inducing the expression of *Kr-h1*, in early instars, whereas its subsequent disappearance allows metamorphosis to occur[2,3,5,13,43,44]. This is because the elevated expression level of *Gb'myo* is essential for the arrest of JH biosynthesis in *G. bimaculatus*[33]. Thus, the shift in the timing of regulation of cross-talk between *Gb'Kr-h1*, *Gb'Br* and *Gb'E93* might be attributed to the mechanism for regulating stepwise expressions of *Gb'myo*.

Gb'Myo and *Gb*'Dpp/*Gb*'Gbb signaling might be associated with the expression of *Gb'Kr-h1*, *Gb'Br-C* and *Gb'E93* through regulating JH biosynthesis. Interestingly, it has previously been demonstrated that *myo* is also expressed in the prothoracic glands (PG) in *G. bimaculatus*[33] and *B. germanica*[45]. Thus, Myo might be independently associated with both JH and ecdysone biosynthesis. Consequently, increased *Gb'E93* expression caused by *Gb'myo* RNAi might be related to changes in 20E level. Thus, *Gb'Kr-h1*, *Gb'Br* and *Gb'E93* are probably regulated by JH and 20E in hemimetabolous *G. bimaculatus*, assuming that *Gb*'Myo and *Gb*'Dpp/*Gb*'Gbb signaling in the CA or *Gb*'Myo signaling in the PG are responsible for regulating JH or ecdysone biosynthesis, respectively.

In this study, we propose a model showing the interactions of *Gb'Kr-h1*, *Gb'Br* and *Gb'E93* during the antepenultimate (sixth) instar (figure 6*a*) with the penultimate (seventh) and final (eighth) nymphal instars (figure 6*b*). First, *Gb'Kr-h1*–dependent repression of *Gb'E93* might be essential for the proper moulting of the penultimate and final nymphal instars, but prevents adult differentiation (figure 6*a*). Subsequently, after moulting into the penultimate nymphal instar, *Gb'E93* represses the expression of *Gb'Kr-h1* and *Gb'Br*; thus, ensuring metamorphosis into adults (figure 6*b*). Therefore, our present results suggest that the expression profiles and the functions of *Gb'Kr-h1*, *Gb'Br* and *Gb'E93* during the sixth–to–penultimate instars of *G. bimaculatus* closely resemble those of the final larval–to–pupal period in holometabolous insects[14,29,41].

Several theories have been proposed to explain the pupal formation and the evolutionary transition from hemimetabolous to holometabolous insects[46,47]. Truman and Riddiford[48,49] proposed a hypothesis that the endocrinology of the larvae of holometabolous insects corresponds to the final hemimetabolous embryonic stage, which the authors termed pronymphs (the pronymph hypothesis). The three stages (pronymph, nymph and adult) of ancestral insect species are equivalent to the larva, pupa and adult stages of insects that exhibit complete metamorphosis. The authors speculated that the progressive changes that occur in a number of nymphal series in basal insects are compressed to a single short period of

morphogenesis that is seen in the larva-to-pupa transition of holometabolous insects. This interpretation might support the pronymph hypothesis[25].

However, this hypothesis is subject to controversy. Huang et al. proposed a hypothesis on the evolution from hemimetaboly to holometaboly regarding *Br* (the wing-to-pupa hypothesis)[26]. In this hypothesis, JH action on *Br* expression shifts from being stimulatory (hemimetaboly) to inhibitory (holometaboly) during the young larval stages. Thus, *Br* expression is inhibited in the young larvae of holometabolous ancestors, suppressing *Br*–dependent wing development and patterning. Accordingly, the roles of *Br* culminated in the morphogenesis of pupae in extant holometabolous species.

In both hypotheses, because *Br* expression is regulated by JH, the evolution of metamorphosis might be attributed to heterochronic change in the timing of JH activation and/or suppression or changes in the target organs of JH action. In addition, *Br* functions might have radically diverged and changed from the progressive development of hemimetabolous nymphs to specifying holometabolous pupa[14,19-22,24-26].

Indeed, we also found that *Gb'Kr-h1* mRNA levels were significantly reduced in *Gb'Br* RNAi-treated sixth instar nymphs. The RNAi knockdown of *Gb'Br* also induced precocious *Gb'E93* expression and promoted precocious adult development in our study. Thus, the expression of *Gb'E93* might be negatively affected by *Gb'Br* in the sixth instar nymphs of *G. bimaculatus*. Therefore, *Gb'Kr-h1* and *Gb'Br* might have to interact for

nymphs to transition to the penultimate instar. However, the phenotypes of *Gb'Br* RNAi knockdown exhibited irregular morphology, especially in the wing pads and ovipositor (electronic supplementary material, figure S2). Nymphs which were given *Gb'Br* RNAi in the third instar showed abnormal development of *Br*-dependent tissues, such as the wing pads in the sixth instar nymphs and the wings and ovipositor in the precocious adults (electronic supplementary material, figure S3). Therefore, the function of *Gb'Br* related to regulating wing size and form is conserved from the progressively nymphal stages in hemimetabolous insects (like *P. apterus*[14], *O. fasciatus*[25] and *B. germanica*[26]) to the final larval stage in holometabolous insects (like *T. castaneum*[19,21], lacewing *Chrysopa perla*[50] and *D. melanogaster*[24]). Interestingly, the role of *Gb'Br* in the wing and ovipositor transition that occurs at the penultimate instar seems similar to those of *Br* in the imaginal leg and eye primordia in the final instar just prior to the onset of their morphogenic growth for metamorphosis in *Manduca sexta*[51]. Thus, *Br* specialises in wing development, and retains the pupal specifying function in these periods. Ultimately, *Gb'Br* is required to prevent adult metamorphosis and to allow the anisometric growth of developing wings and ovipositors in *G. bimaculatus*.

5. Conclusions

We demonstrated that the parallel timing of the critical interaction between *Kr-h1* and *Br* is conserved in hemimetabolous and holometabolous insects. This interaction underlies the transition to the penultimate instar nymph in *G. bimaculatus* and the formation of pupae in holometabolous insects. Thus, these periods might represent evolutionarily homologous units. *Gb'Br* was shown to regulate progressive wing development during nymphal stages. In addition, the interaction between Gb'*Kr-h1* and *Gb'Br* is related to the transition that occurs during later (antepenultimate-to-penultimate) instars, preventing metamorphosis to adults in *G. bimaculatus* (figure 6*a*). In holometabolous insects, *Br* might fulfil both function of regulating wing development and preventing adult metamorphosis in the single short period of pupal transition.

We hypothesize that three stages, pronymph (first postembryonic stage), nymphs, and penultimate nymph, of hemimetabolous insect *G. bimaculatus* are equivalent to the larva, final larva, and pupa stages of insects with complete metamorphosis (figure 6*c*). Notably, the prepupa (late phase of the final larva)-to-pupa transitional stages of holometabolous insects might be evolutionary homologous to the antepenultimate-to-penultimate nymph transitional stages of *G. bimaculatus*, supported by the conservation of the mechanisms underlying insect metamorphosis. In addition, wing formation and development from the larva to the pupa might originate from

the periods of pronymph-to-penultimate nymph in hemimetabolous insects.

References

1 Dubrovsky EB. Hormonal cross talk in insect development. Trends Endocrin Met. 2005;16. Availbale from: doi:10.1016/j.tem.2004.11.003.

2 Truman JW, Riddiford LM. Endocrine insights into the evolution of metamorphosis in insects. Ann Rev Entomol. 2002;47. Available from: doi:10.1146/annurev.ento.47.091201.145230.

3 Jindra M, Palli SR, Riddiford LM. The juvenile hormone signaling pathway in insect development. Ann Rev Entomol. 2013;58. Available from: doi:10.1146/annurev-ento-120811-153700.

4 Riddiford LM, Cherbas P, Truman JW. Ecdysone receptors and their biological actions. Vitam Horm. 2000;60. Available from: doi:10.1016/S0083-6729(00)60016-X.

5 Yamanaka N, Rewitz KF, O'Connor MB. Ecdysone control of developmental transitions: Lessons from Drosophila research. Annu Rev Entomol. 2013;58. Available from: doi:10.1146/annurev-ento-120811-153608.

6 Xu Y, Fang F, Chu Y, Jones D, Jones G. Activation of transcription through the ligand-binding pocket of the orphan nuclear receptor ultraspiracle. Eur J Biochem. 2002;269. Available from: doi:10.1046/j.1432-1033.2002.03293.x.

7 Ashok M, Turner C, Wilson TG. Insect juvenile hormone resistance

gene homology with the bHLH-PAS family of transcriptional regulators. Proc Natl Acad Sci USA. 1998;95. Available from: doi:10.1073/pnas.95.6.2761.

8 Charles JP. et al. Ligand-binding properties of a juvenile hormone receptor, Methoprene-tolerant. Proc Natl Acad Sci USA. 2011;108. Available from: doi:10.1073/pnas.1116123109.

9 Jindra M, Uhlirova M, Charles JP, Smykal V, Hill RJ. Genetic evidence for function of the bHLH-PAS protein Gce/Met as a Juvenile hormone receptor. PLoS Gen. 2015;11. Available from: doi:10.1371/journal.pgen.1005394.

10 Riddiford LM, Truman JW, Mirth CK, Shen YC. A role for juvenile hormone in the prepupal development of Drosophila melanogaster. Development. 2010;137. Available from: doi:10.1242/dev.037218.

11 Kayukawa T. et al. Transcriptional regulation of juvenile hormone-mediated induction of Kruppel homolog 1, a repressor of insect metamorphosis. Proc Natl Acad Sci USA. 2012;109. Available from: doi:10.1073/pnas.1204951109.

12 Smykal V. et al. Importance of juvenile hormone signaling arises with competence of insect larvae to metamorphose. Dev Biol. 2014;390. Available from: doi:10.1016/j.ydbio.2014.03.006.

13 Jindra M, Bellés X, Shinoda T. Molecular basis of juvenile hormone signaling. Curr Opin Insect Sci. 2015;11. Available from:

doi:10.1146/annurev-ento-120811-153700.

14 Konopova B, Smykal V, Jindra M. Common and distinct roles of juvenile hormone signaling genes in metamorphosis of holometabolous and hemimetabolous insects. PloS one. 2011;6. Available from: doi:10.1371/journal.pone.0028728.

15 Minakuchi C., Namiki T, Shinoda T. Kruppel homolog 1, an early juvenile hormone-response gene downstream of Methoprene-tolerant, mediates its anti-metamorphic action in the red flour beetle *Tribolium castaneum*. Dev Biol. 2009;325. Available from: doi:10.1016/j.ydbio.2008.10.016.

16 Minakuchi C, Zhou X, Riddiford LM. Kruppel homolog 1 (Kr-h1) mediates juvenile hormone action during metamorphosis of Drosophila melanogaster. Mechan Dev. 2008;125. Available from: doi:10.1016/j.mod.2007.10.002.

17 Lozano J, Bellés X. Conserved repressive function of Kruppel homolog 1 on insect metamorphosis in hemimetabolous and holometabolous species. Sci Rep. 2011;1. Available from: doi:10.1038/srep00163.

18 Minakuchi C, Tanaka M, Miura K, Tanaka, T. Developmental profile and hormonal regulation of the transcription factors broad and Kruppel homolog 1 in *Hemimetabolous thrips*. Insect Biochem Mol Biol. 2011;41. Available from: doi:10.1016/j.ibmb.2010.11.004.

19 Parthasarathy R, Tan A, Bai H, Palli SR. Transcription factor broad suppresses precocious development of adult structures during larval-pupal metamorphosis in the red flour beetle, *Tribolium castaneum*. Mechan Dev. 2008;125. Available from: doi:10.1016/j.mod.2007.11.001.

20 Uhlirova M. et al. Use of Sindbis virus-mediated RNA interference to demonstrate a conserved role of Broad-Complex in insect metamorphosis. Proc Natl Acad Sci USA. 2003;100. Available from: doi:10.1073/pnas.2136837100.

21 Suzuki Y, Truman JW, Riddiford LM. The role of Broad in the development of *Tribolium castaneum*: implications for the evolution of the holometabolous insect pupa. Development. 2008;135. Available from: doi:10.1242/dev.015263.

22 Konopova B, Jindra M. Broad-Complex acts downstream of Met in juvenile hormone signaling to coordinate primitive holometabolan metamorphosis. Development. 2008;135. Available from: doi:10.1242/dev.016097.

23 DiBello PR, Withers DA, Bayer CA, Fristrom JW, Guild GM. The Drosophila Broad-Complex encodes a family of related proteins containing zinc fingers. Genetics. 1991;129. Available from: PMCID: PMC1204631.

24 Zhou X, Riddiford LM. Broad specifies pupal development and

mediates the 'status quo' action of juvenile hormone on the pupal-adult transformation in Drosophila and Manduca. Development. 2002;129. Available from: PMID:11959833.

25 Erezyilmaz DF, Riddiford LM, Truman JW. The pupal specifier broad directs progressive morphogenesis in a direct-developing insect. Proc Natl Acad Sci USA. 2006;103. Available from: doi:10.1073/pnas.0509983103.

26 Huang JH, Lozano J, Bellés X. Broad-complex functions in postembryonic development of the cockroach *Blattella germanica* shed new light on the evolution of insect metamorphosis. Biochim Biophys Acta. 2013;1830. Available from: doi:10.1016/j.bbagen.2012.09.025.

27 Baehrecke EH, Thummel CS. The Drosophila E93 gene from the 93F early puff displays stage- and tissue-specific regulation by 20-hydroxyecdysone. Dev Biol. 1995;171. Available from: doi:10.1006/dbio.1995.1262.

28 Urena E, Manjon C, Franch-Marro X, Martin D. Transcription factor E93 specifies adult metamorphosis in hemimetabolous and holometabolous insects. Proc Natl Acad Sci USA. 2014;111. Available from: doi:10.1073/pnas.1401478111.

29 Urena E, Chafino S, Manjon C, Franch-Marro X, Martin D. The occurrence of the holometabolous pupal stage requires the interaction

between E93, Kruppel-Homolog 1 and Broad-Complex. PLoS Gen. 2016;12. Available from: doi:10.1371/journal.pgen.1006020.

30 Bellés X, Santos CG. The MEKRE93 (Methoprene tolerant-Kruppel homolog 1-E93) pathway in the regulation of insect metamorphosis, and the homology of the pupal stage. Insect Biochem Mol Biol. 2014;52. Available from: doi:10.1016/j.ibmb.2014.06.009.

31 Bellés X. The origin of insect metamorphosis, the innovation of the final molt, and the MEKRE93 pathway. Phil. Trans. R. Soc. B. 2019;

32 Mito T, Noji S. The two-spotted cricket *Gryllus bimaculatus*: An emerging model for developmental and regeneration studies. CSH Prot. 2008;110. Available from: doi:10.1101/pdb.emo110.

33 Ishimaru Y. et al. TGF-beta signaling in insects regulates metamorphosis via juvenile hormone biosynthesis. Proc Natl Acad Sci USA. 2016;113. Available from: doi:10.1073/pnas.1600612113.

34 Niwa N, Saitoh M, Ohuchi H, Yoshioka H, Noji S. Correlation between distal-less expression patterns and structures of appendages in development of the two-spotted cricket, Gryllus bimaculatus. Zool Sci. 1997;14. Available from: doi:10.2108/Zsj.14.115.

35 Ishimaru Y. et al. Involvement of dachshund and Distal-less in distal pattern formation of the cricket leg during regeneration. Sci Rep. 2015;5. Available from: doi:10.1038/srep08387.

36 Miyawaki K. et al. Involvement of Wingless/Armadillo signaling in

the posterior sequential segmentation in the cricket, Gryllus bimaculatus (Orthoptera), as revealed by RNAi analysis. Mechan Dev. 2004;121. Available from: doi:10.1016/j.mod.2004.01.002.

37 Cao JQ. et al. The Role of MicroRNAs in Drosophila Regulation of Insulin-Like Peptides and Ecdysteroid Signalling: Where Are We Now?. Adv Insect Physiol. 2017;53. Available from: doi:10.1016/bs.aiip.2017.02.002.

38 Mou X, Duncan DM, Baehrecke EH, Duncan I. Control of target gene specificity during metamorphosis by the steroid response gene E93. Proc Natl Acad Sci USA. 2012;109. Available from: doi:10.1073/pnas.1117559109

39 Baehrecke EH, Thummel CS. The Drosophila E93 gene from the 93F early puff displays stage- and tissue-specific regulation by 20-hydroxyecdysone. Dev Biol. 1995;171. Available from: doi:10.1006/dbio.1995.1262.

40 Liu X. et al. 20-Hydroxyecdysone (20E) Primary Response Gene E93 Modulates 20E Signaling to Promote Bombyx Larval-Pupal Metamorphosis. J Biol Chem. 2015;290 Available from: doi:10.1074/jbc.M115.687293.

41 Jindra M. Where dose the pupa come from? The timing of juvenile hormone signalling supports homology between stages of hemimetabolous and holometabolous insects. Phil. Trans. R. Soc. B.

2019;

42 Gujar H, Palli SR. Kruppel homolog 1 and E93 mediate Juvenile hormone regulation of metamorphosis in the common bed bug, *Cimex lectularius*. Sci Rep. 2016;6. Available from: doi:10.1038/srep26092.

43 Riddiford LM. Cellular and molecular actions of juvenile hormone. I. General considerations and premetamorphic actions. Adv Insect Physiol. 1994;24. Available from: doi:10.1016/S0065-2806(08)60084-3.

44 Hiruma K, Kaneko Y. Hormonal regulation of insect metamorphosis with special reference to juvenile hormone biosynthesis. Curr top dev biol. 2013;103. Available from: doi:10.1016/B978-0-12-385979-2.00003-4.

45 Kamsoi O, Bellés X. Myoglianin triggers the premetamorphosis stage in hemimetabolan insects. FASEB J. 2019;33. Available from: doi:10.1096/fj.201801511R.

46 Cheong SP, Huang J, Bendena WG, Tobe SS, Hui JH. Evolution of ecdysis and metamorphosis in arthropods: The rise of regulation of juvenile hormone. Integr Comp Biol. 2015;55. Available from: doi:10.1093/icb/icv066.

47 Bellés X. Origin and evolution of insect metamorphosis. In: Encyclopedia of Life Sciences (eLS). John Wiley & Sons, Ltd., Chichester. 2011, doi:10.1002/9780470015902.a0022854.

48 Truman JW, Riddiford LM. The origins of insect metamorphosis. Nature 1999;401. Available from: doi:10.1038/46737.

49 Truman JW, Riddiford LM. The Evolution of Insect Metamorphosis: A Developmental and Endocrine View. Phil. Trans. R. Soc. B. 2019;

50 Konopova B, Jindra M. Broad-Complex acts downstream of Met in juvenile hormone signaling to coordinate primitive holometabolan metamorphosis. Development. 2008;135. Available from: doi:10.1242/dev.016097.

51 Truman JW. et al. Juvenile hormone is required to couple imaginal disc formation with nutrition in insects. Science 2006;312. Available from: doi:10.1126/science.1123652.

Data accessibility

The datasets supporting this article have been uploaded as part of the supplementary material. *Gb'Kr-h1* (accession number LC476894), *Gb'Br* (accession number LC476892) and *Gb'E93* (accession number LC476893) cDNA sequences have been deposited in DNA Data Bank of Japan.

Authors' contributions

Y.I., S.N. and T.M. designed this study. Y.I. performed all of the experiments. Y.I., S.T., T.W., S.N. and T.M. analysed the data. Y.I., S.N. and T.M. prepared all of the figures and wrote the main text of the manuscript. All of the authors critically assessed the manuscript.

Competing interests

We have no competing interests.

Funding

This work was supported by the Japan Society for the Promotion of Science (JSPS) KAKENHI Grant Number JP16K1506800 to Y.I., JP26292176 to T.M., and JP17H03945 to T.M. and Y.I.

Acknowledgments

We thank Kayoko Tada for providing technical assistance.

Figure Legends

Figure 1. Phenotypes observed after RNAi-mediated depletion of *Gb'Kr-h1* and *Gb'Br* in the nymph stage of *G. bimaculatus*.

(*a*) dsRNA was injected into nymphs on day 1 of the fifth instar. After hatching, the life cycle of cricket nymphs progresses through eight instars, and the final instar nymph moults into an adult. (*b*,*c*) The effects of RNAi targeting *DsRed2* (control), *Gb'Kr-h1* or *Gb'Br* in nymphs on day 1 of the fifth instar. In each panel, the control adult is on the left side and the RNAi-treated on the right. RNAi-treated nymphs underwent precocious adult metamorphosis after the sixth instar. (*d*,*e*) Body length (*d*) and weight (*e*) of adults (male: ♂; and female: ♀) that developed following injections of dsRNA targeting *DsRed2*, *Gb'Kr-h1* or *Gb'Br*. Data are presented as the mean ± SD. *, $P < 0.05$; **, $P < 0.005$ according to Student's *t*-test. (*f*–*i*) Wings of precocious adults produced following the injection of dsRNA were significantly smaller and were wrinkled (*f*–*h*). Following the injection of 20E at the fifth instar, the fifth instar nymphs underwent precocious adult metamorphosis after the sixth instar, and the wings of the 20E-treated adults were also significantly reduced and wrinkled (*i*). (*j*–*m*) Ovipositors of precocious adults produced following the injection of dsRNAs (*j*–*l*) or 20E-treated (*m*) were cleaved at the tip and they became abnormally short. Scale bars: 10 mm in *a*–*c*; 2 mm in *f*–*m*.

Figure 2. Phenotypes observed after *Gb'E93* depletion using RNAi in *G. bimaculatus*.

(*a–c*) dsRNA targeting *DsRed2* (control) or *Gb'E93* was injected into fifth instars on day 1. The fifth instar nymphs that received RNAi targeting *Gb'E93* initiated supernumerary moults at the eighth-ninth-tenth instars (instead of eighth instar to adult), and subsequently developed into large-sized adults compared with the control adults. The nymphal instar and adult stage are indicated at the bottom of each panel (male: ♂; and female: ♀). (*d-f*) Lateral views of the eighth (*d*), adult (*e*), or tenth (*f*) instar nymphs that were injected with dsRNA targeting *DsRed2* or *Gb'E93* on day 1 of the fifth instar, respectively. Magenta arrows indicate the white pigmentation of the head and prothorax. (*g*,*h*) Body length (*g*) and weight (*h*) of adults that were treated with RNAi targeting *DsRed2* or *Gb'E93*. Data are presented as the mean ± SD. *, $P < 0.05$; **, $P < 0.005$; ***, $P < 0.001$ according to Student's *t*-test. (*i*,*j*) Dorsal views of the eighth instar or a representative supernumerary tenth instar nymph that was injected with dsRNA targeting *DsRed2* (*i*) or *Gb'E93* (*j*) on day 1 of the fifth instar. Scale bars: 10 mm in *a–c*; 2 mm in *d–f*, *i*, *j*.

Figure 3. Expression profiles of *Gb'Kr-h1 Gb'Br* and *Gb'E93* transcripts in *Gryllus bimaculatus* during development.

(*a*,*c*,*e*) Temporal expression of *Gb'Kr-h1* (*a*), *Gb'Br* (*c*), and *Gb'E93* (*e*) in the abdomen tissues of nymphs based on qPCR analyses. Relative fold changes in mRNA levels were plotted, and the average expression levels on day 1 of the sixth instar were set at 1. mRNA levels were normalized to *Gb'β-actin* mRNA levels. Developmental stages are defined as days (D) after moulting. Data are presented as the mean ± SD. (*b*,*d*,*f*) Transcript levels of *Gb'Kr-h1* (*b*), *Gb'Br* (*d*), and *Gb'E93* (*f*) were determined on days 1 of the sixth and seventh instars. The transcript levels determined on day 1 of the sixth instar control nymphs were set to 1. The data presented are the mean ± SD. *, $P < 0.05$; **, $P < 0.005$ according to Student's *t*-test. (*g*) Comparison between expression levels of *Gb'Kr-h1*, *Gb'Br*, and *Gb'E93* during the development of nymphs. Units in the ordinates reflect the relative mRNA levels at each moment. Each value measured in individuals on day 1 of the sixth instar were set to 1. The blue, magenta, and green curved lines represent the *Gb'Kr-h1*, *Gb'Br*, and *Gb'E93* mRNA levels, respectively.

Figure 4. Effect of RNAi-mediated knockdown of *Gb'Kr-h1*, *Gb'Br* or *Gb'E93* and 20E-treatment on expression patterns.

(*a–c*) dsRNA targeting *DsRed2* (control), *Gb'Kr-h1*, *Gb'Br*, or *Gb'E93* was injected on day 1 of the fifth instar. Transcript levels of *Gb'Kr-h1* (*a*), *Gb'Br* (*b*) and *Gb'E93* (*c*) were subsequently determined in the abdomens of the sixth instar. The transcript levels determined at the sixth instar of each

control nymph for panels *a–c* were set to 1. Data are presented as the mean ± SD. (*d*) Transcript levels of *Gb'Kr-h1*, *Gb'Br* and *Gb'E93* were also determined for the seventh instar, following the injection of dsRNA targeting *Gb'E93*. The transcript levels of these genes in control nymphs on day 1 of the seventh instar were set to 1. Data are presented as the mean ± SD. (*e*) 20E was injected into the fifth instar nymphs. Transcript levels of *Gb'Kr-h1*, *Gb'Br*, and *Gb'E93* were subsequently determined on days 1 in the sixth instars. The transcript levels of these genes on day 1 of the control sixth instar nymphs were set to 1. Data presented are the mean ± SD. n.s., not significant; *, $P < 0.05$; **, $P < 0.005$; ***, $P < 0.001$ according to Student's *t*-test.

Figure 5. Effects of RNAi-mediated depletion of *Gb'myo* and *Gb'mad* on the expression of *Gb'Kr-h1*, *Gb'Br* and *Gb'E93*.

(*a-c*) *Gb'Kr-h1*, *Gb'Br* and *Gb'E93* mRNA levels in the abdomen of sixth instar nymphs after injecting dsRNA targeting *Gb'myo* or *Gb'mad* into fifth instars. The transcript levels of the control sixth instar nymphs were set to 1. Data are presented as the mean ± SD. *, $P < 0.05$; **, $P < 0.005$ according to Student's *t*-test.

Figure 6. Schematics of the mechanisms regulating adult characteristics in the hemimetabolous insect *G. bimaculatus*.

(*a*,*b*) Schematic diagrams of the regulatory mechanisms in controlling adult differentiation[29] based on the results obtained from experiments targeting *Gb'Kr-h1*, *Gb'Br*, and *Gb'E93* genes using RNAi. The proposed models depict the regulatory interaction between these metamorphic genes in the antepenultimate (sixth), penultimate (seventh) and final (eighth) nymphal instars of *G. bimaculatus*. Grey colours denote gene depletion and transcriptional regulatory effects that are absent during each phase. Magenta and blue lines indicate the findings of the present study. The characters illustrating the functions of TGF-β signaling in controlling JH biosynthesis are from *G. bimaculatus*[33]. The role of 20E still remains unclear (dotted lines). (*c*) Schematic of the hypothesis for the stages of ancestral insects, holometabolous insects and hemimetabolous (*G. bimaculatus*) counterparts[46,49]. Magenta arrows indicate the periods of *Br* expression in holometabolous insects and *G. bimaculatus*.

dsRNA	n	Nymphal mortality	Adult hallmark after 6th	Adult hallmark after 7th	Normal adult
Control	43	2 (4.7%)	0 (0%)	0 (0%)	41 (95.3%)
Gb'Kr-h1	39	12 (30.8%)	15 (38.5%)	4 (10.2%)	8 (20.5%)
Gb'Br	31	6 (19.4%)	24 (77.4%)	0 (0%)	1 (3.2%)

dsRNA	n	Nymphal mortality	Supernumerary molt		Normal adult
			10th	adult	
control	38	3 (7.9%)	0 (0%)	—	35 (92.1%)
Gb'E93	39	14 (35.9%)	25 (64.1%)	8 (20.5%)	0 (0%)

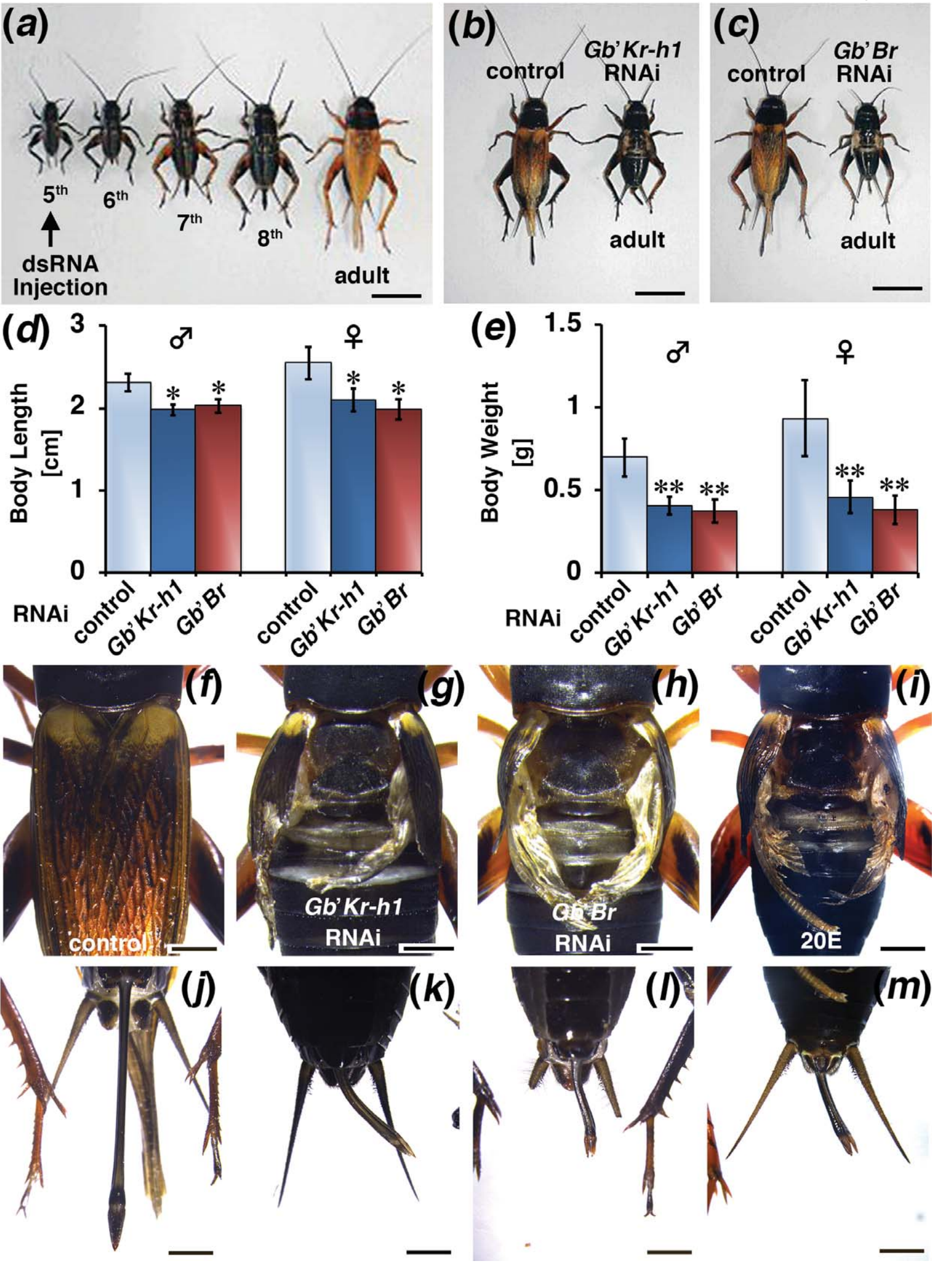
(a)
5th
6th
7th
8th
adult
dsRNA Injection
(b)
control
Gb'Kr-h1 RNAi
adult
(c)
control
Gb'Br RNAi
adult
(d)
♂
♀
Body Length [cm]
3
2
1
0
*
RNAi
control
Gb'Kr-h1
Gb'Br
(e)
♂
♀
Body Weight [g]
1.5
1
0.5
0
**
RNAi
control
Gb'Kr-h1
Gb'Br
(f)
control
(g)
Gb'Kr-h1 RNAi
(h)
Gb'Br RNAi
(i)
20E
(j)
(k)
(l)
(m)

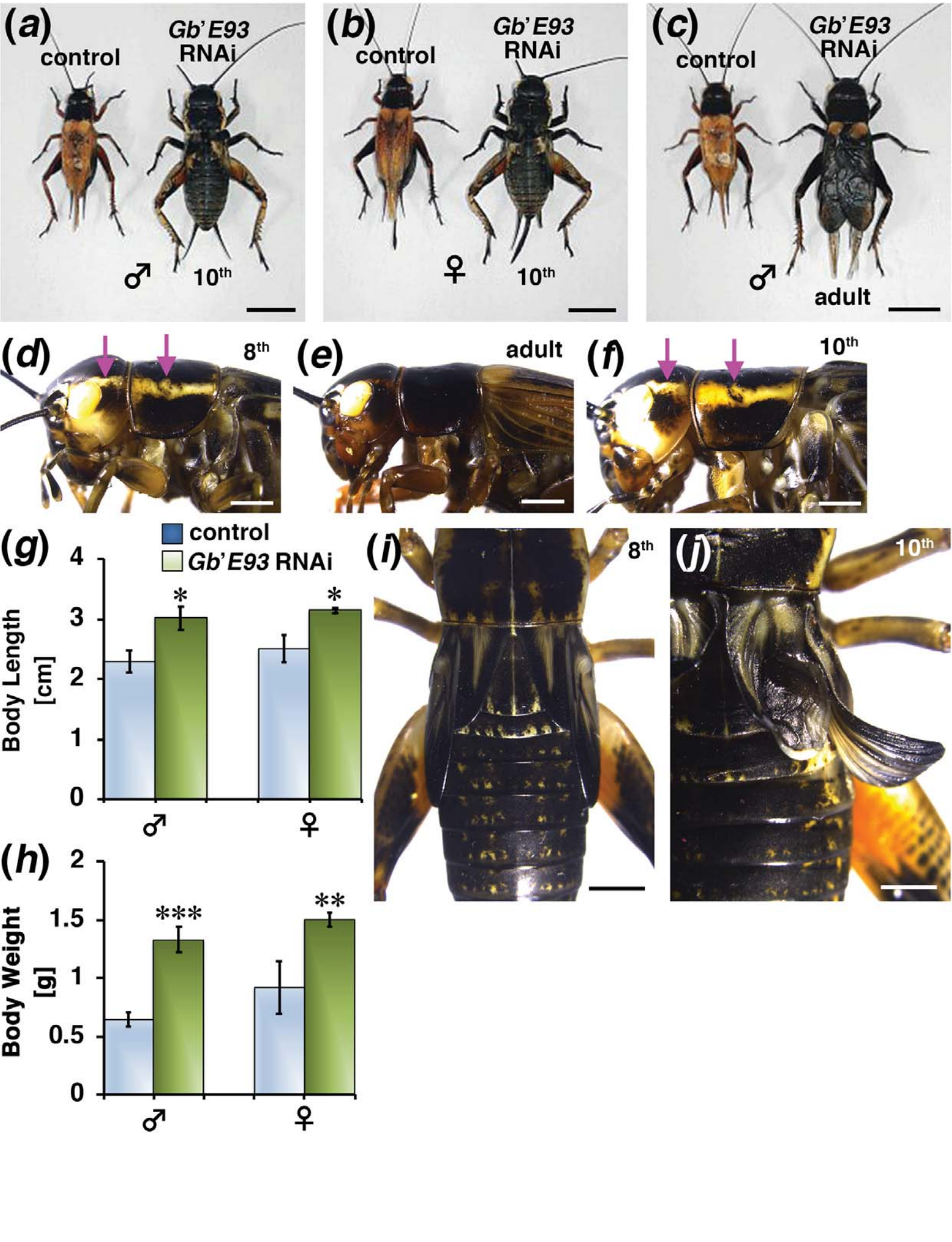
(a)
control
Gb'E93 RNAi
♂
10th
(b)
control
Gb'E93 RNAi
♀
10th
(c)
control
Gb'E93 RNAi
♂
adult
(d)
8th
(e)
adult
(f)
10th
(g)
control
Gb'E93 RNAi
Body Length [cm]
0
1
2
3
4
*
*
♂
♀
(h)
Body Weight [g]
0
0.5
1
1.5
2
***
**
♂
♀
(i)
8th
(j)
10th

Figure 3

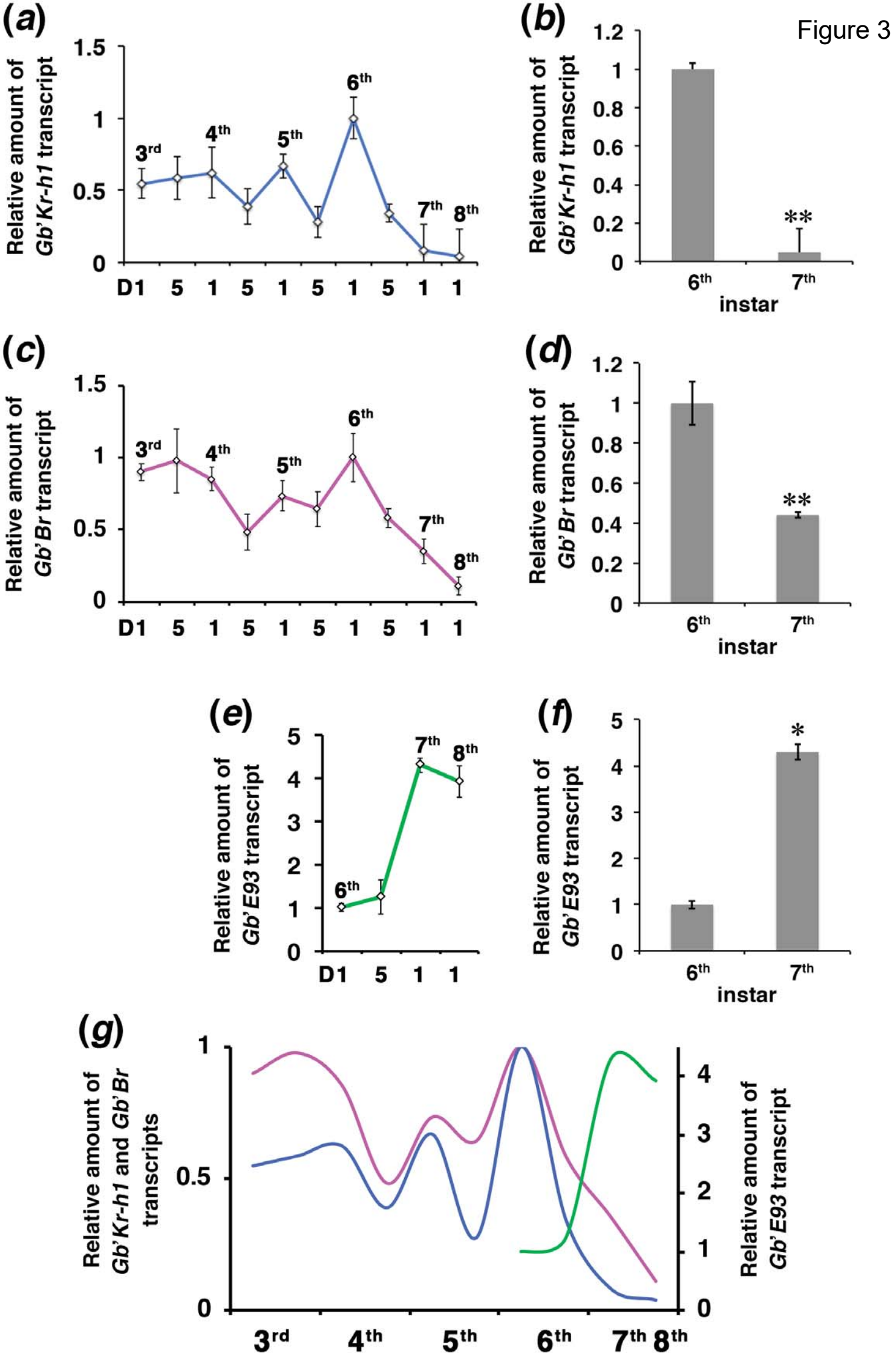
(a)
Relative amount of Gb'Kr-h1 transcript
1.5
1
0.5
0
3rd
4th
5th
6th
7th
8th
D1 5 1 5 1 5 1 5 1 1
(b)
Relative amount of Gb'Kr-h1 transcript
1.2
1
0.8
0.6
0.4
0.2
0
**
6th
7th
instar
(c)
Relative amount of Gb'Br transcript
1.5
1
0.5
0
3rd
4th
5th
6th
7th
8th
D1 5 1 5 1 5 1 5 1 1
(d)
Relative amount of Gb'Br transcript
1.2
1
0.8
0.6
0.4
0.2
0
**
6th
7th
instar
(e)
Relative amount of Gb'E93 transcript
5
4
3
2
1
0
6th
7th
8th
D1 5 1 1
(f)
Relative amount of Gb'E93 transcript
5
4
3
2
1
0
*
6th
7th
instar
(g)
Relative amount of Gb'Kr-h1 and Gb'Br transcripts
1
0.5
0
Relative amount of Gb'E93 transcript
4
3
2
1
0
3rd
4th
5th
6th
7th
8th

Figure 4

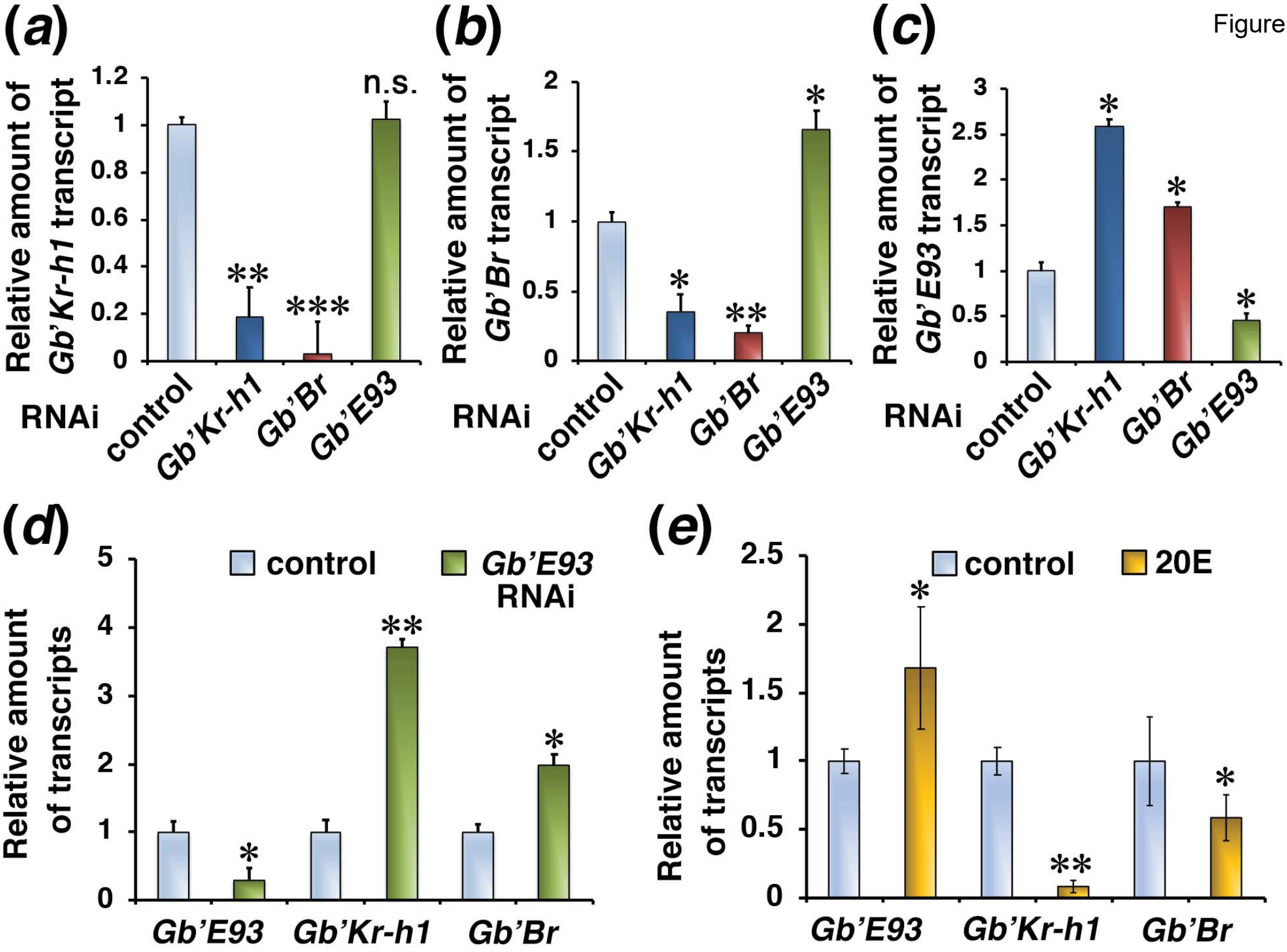
(a)
Relative amount of Gb'Kr-h1 transcript
1.2
1
0.8
0.6
0.4
0.2
0
**
***
n.s.
RNAi
control
Gb'Kr-h1
Gb'Br
Gb'E93
(b)
Relative amount of Gb'Br transcript
2
1.5
1
0.5
0
*
**
*
RNAi
control
Gb'Kr-h1
Gb'Br
Gb'E93
(c)
Relative amount of Gb'E93 transcript
3
2.5
2
1.5
1
0.5
0
*
*
*
RNAi
control
Gb'Kr-h1
Gb'Br
Gb'E93
(d)
Relative amount of transcripts
5
4
3
2
1
0
control
Gb'E93 RNAi
*
**
*
Gb'E93
Gb'Kr-h1
Gb'Br
(e)
Relative amount of transcripts
2.5
2
1.5
1
0.5
0
control
20E
*
**
*
Gb'E93
Gb'Kr-h1
Gb'Br

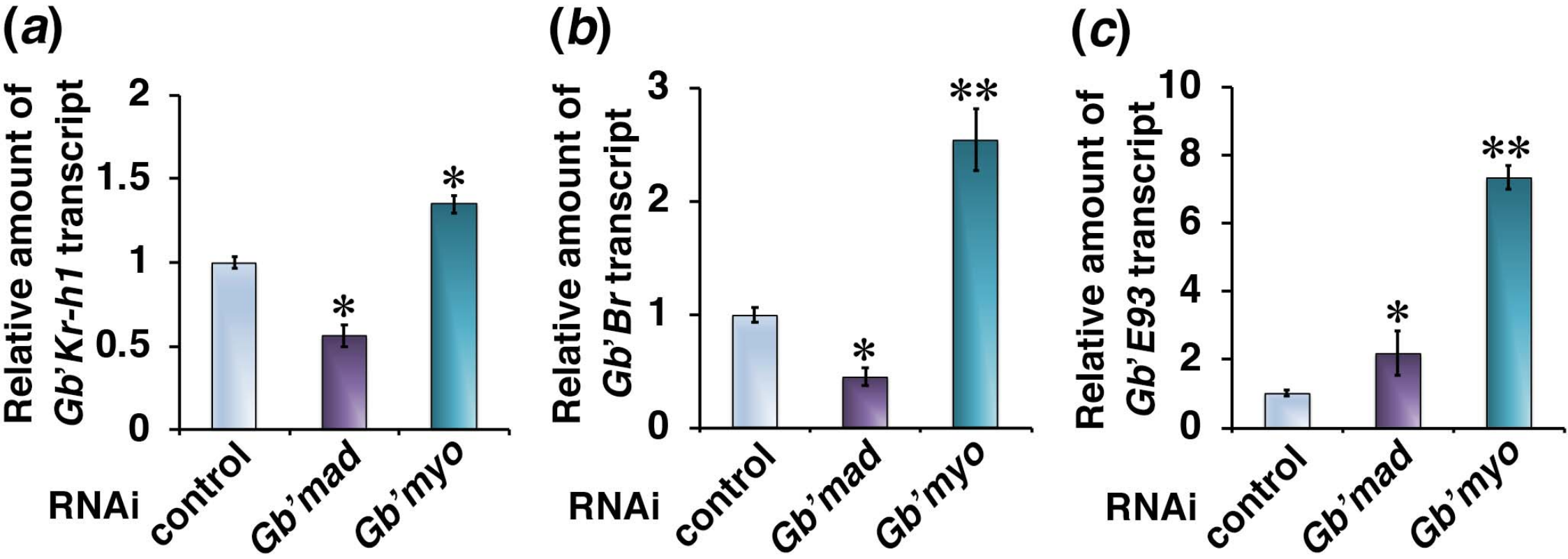
(a)
Relative amount of Gb'Kr-h1 transcript
2
1.5
1
0.5
0
*
*
RNAi
control
Gb'mad
Gb'myo
(b)
Relative amount of Gb'Br transcript
3
2
1
0
*
**
RNAi
control
Gb'mad
Gb'myo
(c)
Relative amount of Gb'E93 transcript
10
8
6
4
2
0
*
**
RNAi
control
Gb'mad
Gb'myo

Figure S1

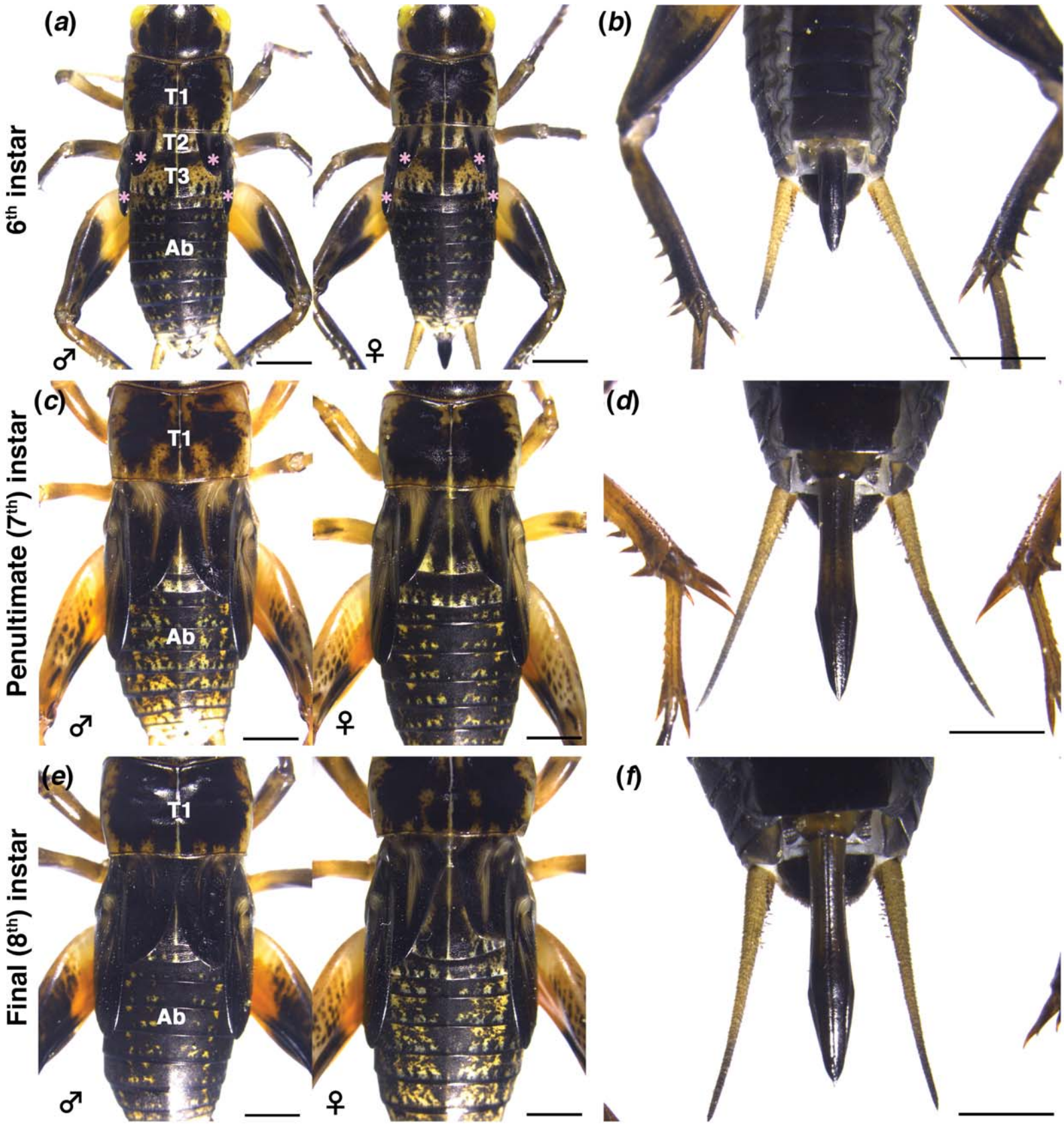
(a)
(b)
(c)
(d)
(e)
(f)
T1
T2
T3
Ab
♂
♀
6th instar
Penultimate (7th) instar
Final (8th) instar

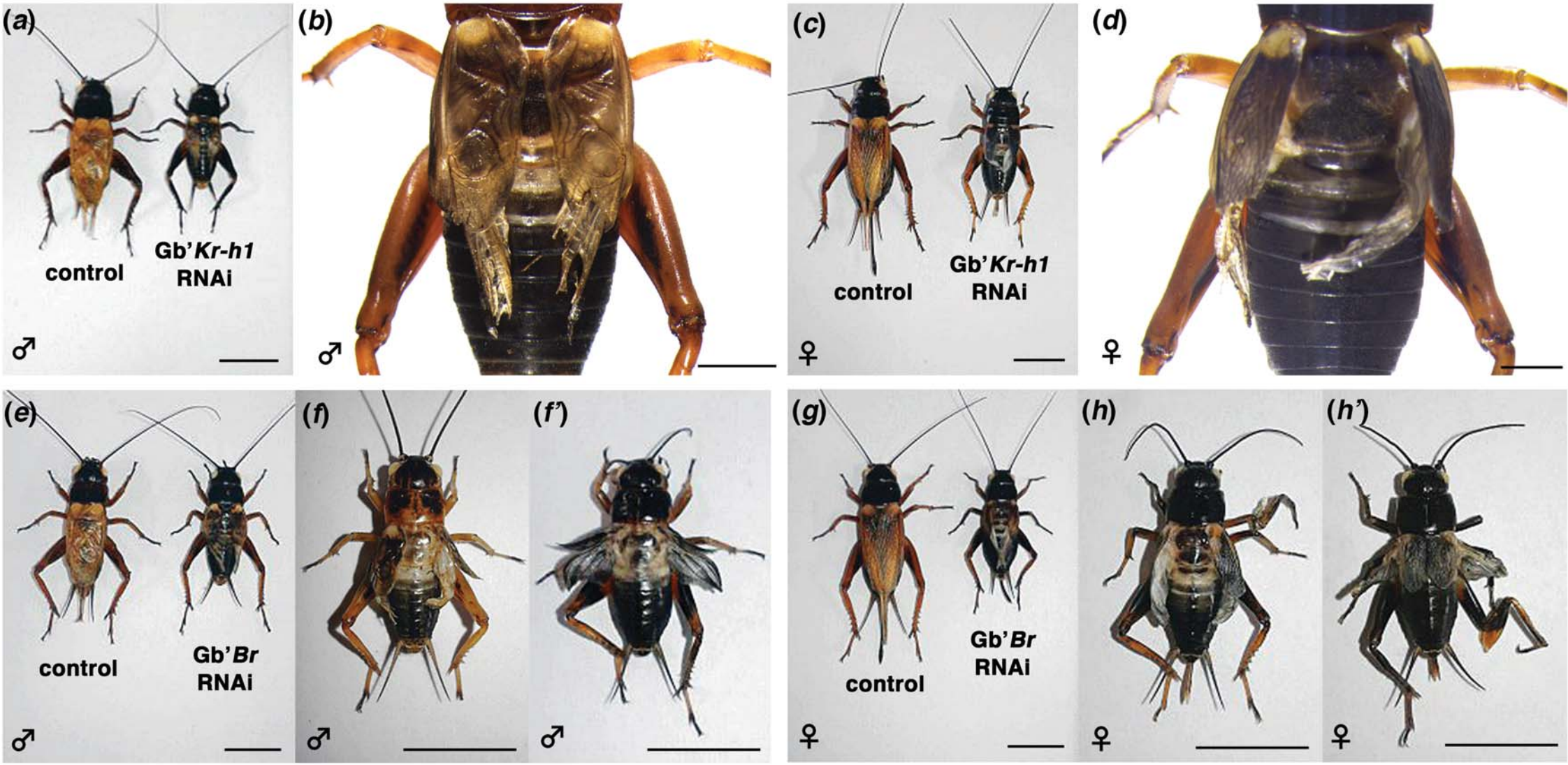
(a)
control
Gb'Kr-h1
RNAi
♂
(b)
♂
(c)
control
Gb'Kr-h1
RNAi
♀
(d)
♀
(e)
control
Gb'Br
RNAi
♂
(f)
♂
(f')
♂
(g)
control
Gb'Br
RNAi
♀
(h)
♀
(h')
♀

Figure S3

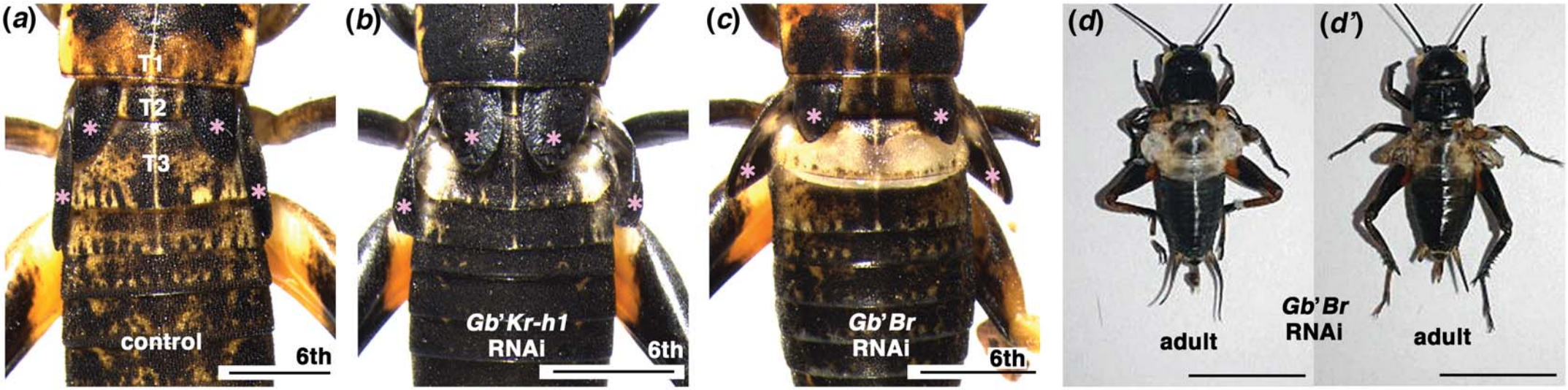
RNAi
3rd injection
(a)
T1
T2
T3
control
6th
(b)
Gb'Kr-h1
RNAi
6th
(c)
Gb'Br
RNAi
6th
(d)
adult
Gb'Br
RNAi
(d')
adult